Alexandria Engineering Journal (2022) 61, 9609–9621

HOSTED BY

ELSEVIER

Alexandria University

Alexandria Engineering Journal

www.elsevier.com/locate/aej
www.sciencedirect.com

Hydrophobic silica sand ceramic hollow fiber membrane for desalination via direct contact membrane distillation

Saber Abdulhamid Alftessi [a], Mohd Hafiz Dzarfan Othman [a,*], Mohd Ridhwan Bin Adam [a], Twibi Mohamed Farag [a], Zhong Sheng Tai [a], Yusuf Olabode Raji [a], Mukhlis A Rahman [a], Juhana Jaafar [a], Ahmad Fauzi Ismail [a], Suriani Abu Bakar [b]

[a] *Advanced Membrane Technology Research Centre (AMTEC), School of Chemical and Energy Engineering (FCEE), Universiti Teknologi Malaysia, 81310 UTM Skudai, Johor, Malaysia*
[b] *Nanotechnology Research Centre, Faculty of Science and Mathematics, Universiti Pendidikan Sultan Idris, 35900 Tanjung Malim, Perak, Malaysia*

Received 7 January 2022; revised 14 March 2022; accepted 18 March 2022
Available online 28 March 2022

KEYWORDS

Hydrophobic;
Ceramic membrane;
Silica sand;
Water desalination;
Membrane distillation

Abstract A porous hollow fibre ceramic membrane derived from a low-cost natural material (silica sand) and fabricated by combine phase inversion and sintering technique followed by fluoroalkylsilane (FAS17) grafting to improve its hydrophobicity is reported in this study. Prior to the subjection of the silica sand ceramic hollow fibre membrane (SSCHFM) to a desalination performance test via direct contact membrane distillation (DCMD), characterization studies were performed on the SSCHFM before and after grafting using different characterization techniques, such as scanning electron microscopy (SEM), atomic force microscopy (AFM), 3-points bending, water liquid entry pressure (LEPw), and water contact angle measurement. Mercury porosimetry analysis (MIP) was also used to determine the pore size distribution and porosity of the SSCHFM. The grafting process caused an increasing of the contact angle from 0° to 142.5° ± 2.0, and LEPw value of (2.6 ± 0.4 bar) was achieved. AFM images showed an increment in the surface roughness of the grafted SSCHFM from 0.305 µm to 0.375 µm, with a slight decrease in the average pore size and porosity from 0.17 µm and 17% to 0.12 µm and 14.7% respectively. After the grafting process, the performance of the membrane in DCMD was evaluated on a salt solution for 32 h at different NaCl concentrations (8,16, 24, 32 and 40) g/L, feed flow rates and feed temperatures. The results showed a decrease in the permeate flux at increasing feed concentration, but the reverse was at higher feed flow rates and feed temperatures. The surface-modified membrane recorded a water flux

* Corresponding author.
E-mail address: hafiz@petroleum.utm.my (M. Hafiz Dzarfan Othman).
Peer review under responsibility of Faculty of Engineering, Alexandria University.

https://doi.org/10.1016/j.aej.2022.03.044

value of 35 $kg/m^2 \cdot h$ and 100% salt rejection. The results indicate that the hydrophobic hollow fibre ceramic membranes derived from silica sand have significant potential to be developed for membrane distillation application in water purification and reclamation.

1. Introduction

Natural freshwater supplies are deficient in many nations worldwide; this situation has been exacerbated by the increasing freshwater demand caused by global population expansion and industrial/agricultural activity. Natural sources of fresh water, such as groundwater and rivers, are currently unable to fulfil rising demand and are depleting at an alarming rate. The freshwater demand in many parts of the world is currently being met via dependence on desalination technologies, especially in the Middle East, where seawater desalination accounts for the significant freshwater source in countries like Saudi Arabia, Kuwait, and the United Arab Emirates [1,2].

Membrane distillation (MD) processes as an alternative solution to the current seawater desalination-related issues. Being a thermal process, MD relies on the use of porous hydrophobic membranes that allows only the passage of water vapor rather than the liquid feed [3]. MD technology can be operated in four different configurations based on the arrangement of the cold side of the system; these include (i) vacuum membrane distillation (VMD), (ii) direct contact membrane distillation (DCMD), (iii) air gap membrane distillation, and (iv) sweeping gas membrane distillation (SGMD) [4]. Among these, DCMD remains the most employed seawater desalination configuration because it is easy to set up at a low cost and its simple design and operation [5].

In the term of membrane materials, the most commonly used membranes for water and wastewater treatment are made of polymeric material, such as polyvinylidenefluoride (PVDF) [6–8], polypropylene (PP) [9] and polytetrafluoroethylene (PTFE) [10,11]. However, there are several issues associated with the use of polymers, such as the incapability to act in some extreme conditions (such as high temperature) and chemical resistance, which is one of the most required properties in MD.

Ceramic membranes represent another class of separators and are famous for their high mechanical strength, chemical and thermal stabilities beside their high flux. Ceramic membranes exhibit significant potential in wastewater treatment [12-14]. Therefore, in recent years, ceramic membranes have attracted much interest in MD processes [15-18]. Despite the many advantages of ceramic membranes, they are still of limited use, especially in large-scale systems, due to the higher cost of ceramic membranes, which discourages widespread use [19].

Alumina, titania, silica and zirconia are common materials for ceramic membrane fabrication; however, using such materials as starting up material is associated with certain drawbacks due to the high sintering temperature that is required to obtain satisfactory results between the mechanical strength and the required porosity, thereby making the final product extremely expensive. Furthermore, alumina, titania, silica and zirconia powders are costly materials; Therefore, many studies were reported to lower the capital costs [20-24]. However, it is likely to be a pioneer in the future with the lower cost of capital.

Meanwhile, the available ceramic membranes are hydrophilic in nature, and this is the major obstacle to their usage; they require a surface modification process with hydrophobic materials such as fluoroalkylsilane (FAS) to improve their hydrophobicity. The hydrophobic surface modification process was first performed by Larbot et al. [25] when they reported a successful modification of a tubular zirconia and alumina hydrophilic membrane into hydrophobic for desalination purposes; the modified membrane exhibited a contact angle of about 150°, while the salt rejection rate and permeate flux were ~ 100% and 8.41 $kg/m^2 \cdot h$ respectively. These results have shown the potential of ceramic membranes to be used in membrane distillation processes rather than relying mainly on polymeric membranes. Hydrophobic ceramic membrane using kaolin for arsenic removal from aqueous solution via DCMD was recently reported [26], the fabricated membrane was modified by grafting with fluoroalkylsilane (FAS) molecules, the study showed a permeate flux of 28 and 25 $kg/m^2 \cdot h$ for As (III), and As (V) respectively, with 100% arsenic rejection was obtained at a feed temperature of 60 °C.

Several investigations have concentrated on fabricating low-cost kaolinite membranes by phase inversion with a high loading concentration due to kaolinite's low density of 2.4 g/cm^3 compared to 3.95 and 4.23 g/cm^3 for alumina and titania, respectively [27,28]. The low density of kaolinite can impede the preparation of dope suspension with a higher loading, particularly when it exceeds 45 wt%. Notably, the optimal dope ceramic content for fabricating well-structured membranes with a narrow pore size distribution and small pore diameters is between 50 and 60 wt% [29]. In a recent study, Twibi et al. [16] have addressed the disadvantage of the low density of kaolinite by converting the kaolinite into mullite-kaolinite using a calcination process at 1300 °C to increase the density of kaolinite from 2.4 g/cm^3 to the range of 3.11–3.26 g/cm^3. However, high calcination temperatures increase the production costs and diminishes the material's low-cost benefit.

Saudi red clay, tetraethyl orthosilicate, ammonia, and sodium alginate powder as a binder were used to fabricate a ceramic membrane for MD. The prepared membrane was tested using sodium chloride solutions and hot raw well water. An average flux of 13.10 $kg/m^2 \cdot h$ was obtained with 98.96% rejection using raw well water [17]. Das et al. [30] developed cost-effective hydrophobic membranes based on clay and alumina in MD. The study obtained 99.96% salt rejection, and a vapour permeate flux of 4.11 $kg/m^2.h$ at a feed temperature of 60 °C. Hubadillah et al. [31] reported a high water flux of 38.2 $kg/m^2.h$ and salt rejection up to 99.9% obtained via DCMD using a surface grafted ceramic membrane prepared from rice husk ash. However, using rice husk ash involves the conversion of rice husk into powder form (silica) through calcination process [20]. One problem with this conversion process via calcination is that the process requires a high calcination temperature of up to 1000 °C to turn the waste material into crystalline silica; this adds to the production cost and annuls the advantage of being low-cost material. In general, using agricultural wastes such as sugarcane bagasse and corn cob ashes [32,33] as a source of silica for green ceramic membranes fabrication reported some drawbacks, i.e. the low melting point of SiO_2 derived from agricultural waste, where the melting point ranges around 700–1000 °C [34]. The material's low melting point leads to an early occurrence of the melting mechanism at a relatively low sintering temperature from 1050 to 1300 °C [35], which impedes reaching satisfactory mechanical strength before the melting of the membrane occurs. Moreover, the high percentage of impurities in the agricultural wastes reduces the silica content (60–90%) [15,23,36], necessitating pre-treatment such as calcination at high temperatures to reduce the impurities level and increase the content of silica.

Previously, we have reported the separation of oil from water using ceramic membrane prepared from natural silica sand via a combined phase inversion and sintering technique [23]. Silica sand is an alternative ceramic material from natural resources that exist in nature. It has a high silica purity of up to 99.5% and high melting point of 1710 °C compared to ranges around 700–1000 °C for the SiO_2 obtained from agriculture waste. As such, silica sand has various attributes that makes it ideal for water filtration; such attributes include high acidic chemical resistance and high hardness. These attributes enhance the mechanical strength of silica sand and are the most effective attributes of filters used in membrane distillation.

Until now, the use of silica sand to fabricate a hydrophobic ceramic hollow fibre membrane for MD applications is yet to be reported. Hence, this work aims to evaluate the possibility of producing SSCHFM from low-cost material for DCMD-based salt solution desalination. The preparation of SSCHFM in this study was done at a sintering temperature of 1300 °C due to its sufficient mechanical strength and suitable pore size in the microfiltration range which was investigated in our previous work [23]. The produced SSCHFM was subjected to a surface modification process with FAS17 for its surface transformation from hydrophilic to hydrophobic. Furthermore, characterization studies were performed on the fabricated and modified SSCHFM using various techniques, such as SEM, AFM, and contact angle measurements. The performance of the surface-modified SSCHFM in DCMD was evaluated in a salt solution, which served as the feed solution, while the stability study was performed at high salinity (8 g/L NaCl) feed solution for 32 h.

2. Experimental

2.1. Materials

In this work, the material used (silica sand powder) has a purity level of 99.5% and 1.6 μm average particle size. Before being used as the starting material, the powder was oven-dried overnight. The polymer binder used was polyethersulfone (PESf), while N-methyl-2-pyrrolidone (NMP) (HPLC grade, Rathbone) served as the solvent; meanwhile, the dispersant used was polyethyleneglycol 30-dipolyhydroxystearate (Arlacel P135, Uniqema). Distilled water and tap water served as the bore fluid and the coagulant bath, respectively, during the spinning process. 97% 1H,1H,2H,2H-perfluorodecyltrie thoxysilane (FAS17) was the grafting agent. NaCl and ethanol (99.5%) were procured from Merck, Germany.

2.2. Silica sand hollow fibre ceramic membrane preparation

As described in our previous work [23], the preparation of the SSCHFM from natural silica sand in this work was done using a phase inversion/sintering technique. A mixture of Arlacel P135 (1 wt%) and NMP (37.12 wt%) was gently stirred, followed by the addition of silica sand powder (55 wt%). Then, the mixture was subjected to a ball mill process executed for 48 h at 196 rpm before adding in 6.56 wt% of PESf. The milling step was conducted for 48 h, after which the degassing process was performed for about 30 min to remove trapped air. After the degassing process, the mixture was extruded through a stainless-steel syringe. Table 1 illustrates the conditions of the spinning process; this extrusion process produced the SSCHFM precursors, which were then immersed in a water coagulation bath for 24 h to get rid of residual solvent. The precursor was later air-dried and sintered in a tubular furnace at a specifically targeted sintering temperature. The sintering temperature was steadily raised to 600 °C at the heating rate of 2 °C/min; the temperature was held for 2 h at 600 °C to ensure complete removal of the organic materials and the polymer binder. A further increase in temperature to 1300 °C was done at 3 °C/min heating rate and held for 3 h. Lastly, the temperature of the process was reduced to an ambient level at 5 °C/ min cooling rate.

2.3. Surface grafting of SSCHFM

The prepared SSCHFM was surface-modified by first washing it with a water–ethanol mixture (ratio 2:1), followed by oven drying at 100 °C. Then, the SSCHFM was submerged in a grafting solution that made up of fluoroalkylsilane $C_{16}H_{19}F_{17}O_3Si$ (FAS17) (2 wt%) and ethanol (98 wt%) for 24 h [31], then rinsed in distilled water before the last drying step in the oven. After the drying step, the prepared membrane was assembled into a membrane module.

Table 1 Composition of the dope Suspension and the spinning parameters.

Composition of the dope Suspension (wt.%)	
Silica sand powder	55
Polyethersulfone (PESf)	6.88
N-methyl-2-pyrrolidone (NMP)	37.12
Arlacel	1
Spinning parameters	
Flow rate of the bore fluid (mL/min)	10
Flow rate of the dope extrusion (mL/min)	6
The air gap distance (cm)	5
Outer diameter of the spinneret (mm)	2
Inner diameter of the spinneret (mm)	1
The utilized bore fluid	Distilled water
The utilized coagulant	Tap water

2.4. Membrane characterization

Scanning electron microscopy (SEM) was employed to visualize the surface view of the prepared SSCHFM before and after surface modification. The SSCHFM was supported on a metal base and scanned to capture the outer surface images. Prior to the scanning process, the samples were first sputtered with platinum. Atomic force microscopy (AFM) was used to evaluate the samples for surface roughness. For this investigation, a portion of the sample was mounted on a metal base, and a total outer surface size of 10 × 10 μm was scanned. The observed roughness of the membrane surface was presented as the mean value of different surface roughness measurements (R_a).

Furthermore, the prepared SSCHFM was also subjected to a hydrophobicity study to determine the water liquid entry pressure (LEPw) and contact angle. A contact angle goniometer was used for the contact angle measurement; this was done using the sessile drop method that requires 2 μL of distilled water. A minimum of 4 measurements was taken for each sample at different spots. Regarding LEPw, the surface-modified SSCHFM was mounted to an adapter; one of its ends was sealed, while an epoxy potting was used to connect the other end to a tubing. Then, water was pumped on the surface of the SSCHFM and observed for the pressure reading when the first water droplet was observed from the lumen side. The pressure reading was considered the LEPw. According to the Laplace-Young Equation (1), the LEPw value depends on the surface tension of the penetrated liquid, the contact angle and the pore size of the membrane. Therefore, the relationship between the LEPw value and the membrane contact angle is given thus:

$$LEPw = \frac{2\gamma_l}{r_{max}} \cos\theta_{ef} \tag{1}$$

where the liquid surface tension is given as γ_l and maximum radius of the pores of the membrane is given as $rmax$; θ_{ef} represents the value of the membrane contact angle.

A mercury porosimetry analysis (MIP) was employed to determine the pore size distribution and porosity of the SSCHFM before and after the surface modification process. The MIP principle relies on the capillary law governing liquid permeation into tiny pores by non-wetting liquid like mercury. MIP was performed in this study using (Micromeritics AutoPore IV 9500 Series, USA).

2.5. Direct contact membrane distillation (DCMD) tests

Fig. 1 shows the lab-scale setup for the DCMD tests in this study. This setup is comprised of hot and cold cycles that are linked to a membrane module. The membrane module has 5 hollow fibres of 0.0012 m^2 total nominal surface area. The system's design was done to support two circulating streams, namely the hot feed stream that flows through the shell side of the membrane and the cold stream that flows through the membranes lumen-side. Different concentrations (8–40 g/L) of NaCl solution were used as the feed on the hot side while the cold side was fed with deionized water. The feed side temperature and flow rate ranged from 50 to 90 °C and 10–60 L/h, respectively. The temperature control of the hot and cold streams was achieved using a coiled heater and a chiller. Temperature measurements for both streams were done using 4 digital thermometers at the inlet and outlet of the module, and a flow rate of 12 L/h was maintained for the cold stream. A weighing balance was used to measure the weight of the cold-water tank, while equation (2) was used to calculate the permeate flux.

$$Jv = \frac{\Delta W}{A\Delta t} \tag{2}$$

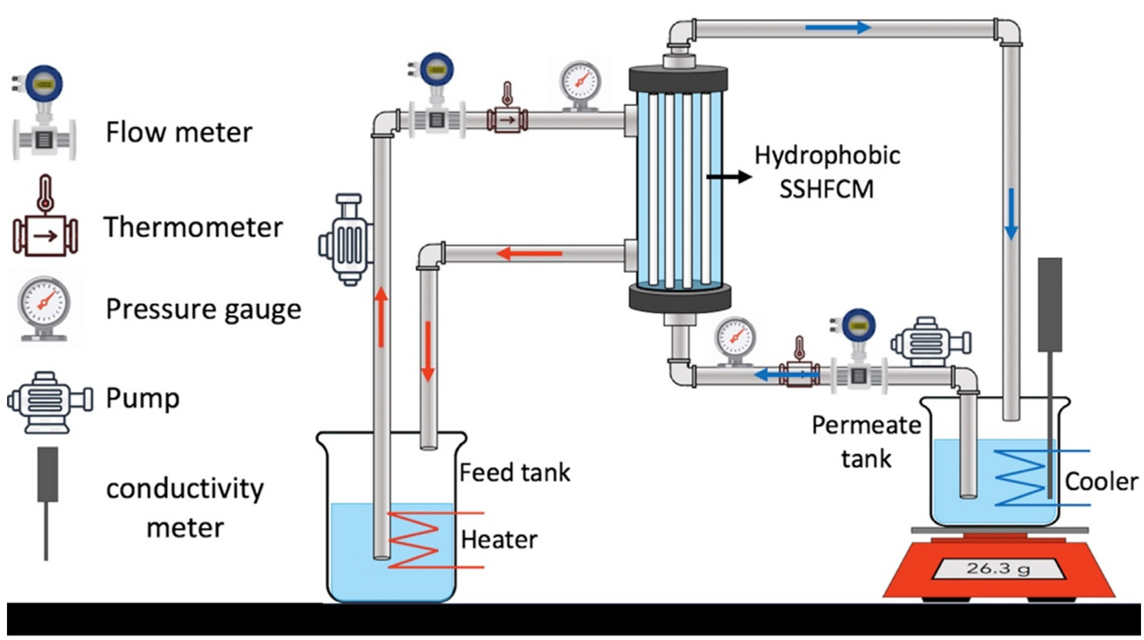

Fig. 1 DCMD laboratory-scale setup.

where ΔW = Change in the cold tank weight (kg) with time (h), A = total effective area of the membranes (0.0012 m^2). the calculation of the salt rejection rate (R%) was done thus:

$$R(\%) = \left(1 - \frac{C_P}{C_F}\right) \times 100\% \tag{3}$$

where R is the NaCl rejection, C_P is the conductivity of the permeate (μs/cm), and C_F is the conductivity of the feed solution (μs/cm); both are measured using a conductivity meter.

3. Results and discussion

3.1. Impact of surface functionalization on the physical properties of SSCHFM

The presence of OH– groups in SSHFCMs confirmed their hydrophilicity properties. Thus, these membranes are not suitable to be applied in MD processes. Therefore, a surface modification step is necessary before SSHFCMs applied in MD processes [3,37].The SEM images of the cross-section and surface of the prepared SSCHFM are shown in Fig. 2, (a) and (b) illustrating the membrane's cross-section area. While (c) and (d) are the views of the external surface of the porous membranes before and after the functionalization step, respectively. Fig. 3 depicting the membrane surface grafting process [38,39]. Evidently, The grafted and non-grafted membranes showed insignificant difference in the SEM images, just that the FAS molecules attached to the membrane surface. This is further corroborated by the increase in surface roughness (Fig. 5), due to the increased number of OH– groups as earlier reported in the literature [40-42].

The properties of the prepared SSCHFM before and after the grafting process are presented in Table 2. The hydrophobicity of the sample was evaluated by measuring the contact angle of a water drop. From the results shown in Table 2, the non-grafted membrane showed no contact angle due to the hydrophilic nature of the sample but exhibited a contact angle value of 142.5° upon grafting process, suggesting its hydrophobicity. The water drop on the membrane surface after grafting is shown in Fig. 4. This observation is in good agreement with previous studies on FAS-based ceramic membranes hydrophobization for MD processes [43-45].

The Laplace-Young Equation is used to express the pressure difference between liquid–vapour interfaces. LEP refers to the minimum hydrostatic pressure value difference needed for the penetration of the feed liquid into the larger membrane pores. This pressure difference is contributed by the interfacial tension, the liquid contact angle at the pore entrance, and the shape and size of the membrane pores [46]. The LEPw of the grafted sample, as shown in Table 2, was 2.6 bar which was significantly higher than the value (0.5 bar) reported by Hubadillah et al. [31]. Das et al. have reported the significant role of the pore size of hydrophobic membranes in sustaining the high LEPw value [30]. For instance, studies by Mulder and Wu [47,48] have suggested that the hydrophobic membrane materials have an optimum pore size. According to Table 2, the grafted sample exhibited a decline in pore size (sponge-like layer) and porosity after grafting from 0.17 to 0.12 μm and 17 to 14.7%, respectively. It is worth noting that the

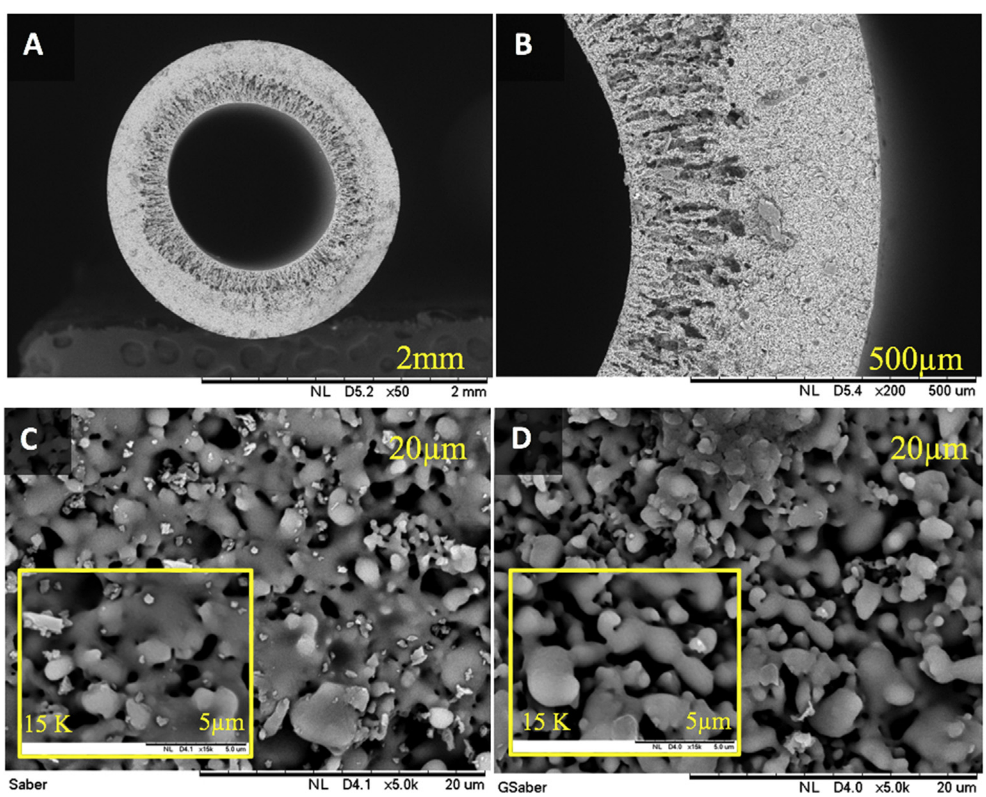

Fig. 2 SEM image of SSCHFM: (a) Cross-sectional view, (b) Higher magnification of cross-sectional view, (c) external surface view prior to grafting, and (d) external surface view after grafting.

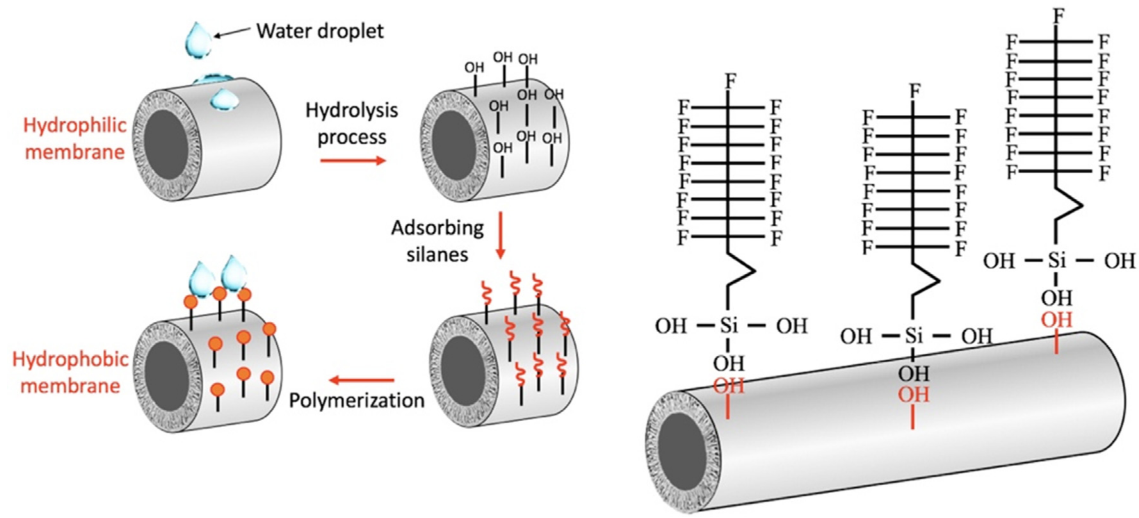

Fig. 3 The depiction of the membrane surface grafting process.

Table 2 Properties of ungrafted and grafted SSCHFM.

Properties	Ungrafted	Grafted
Contact angle (°)	0	142.5 ± 2.0
LEPw (bar)	1.1 ± 0.1	2.6 ± 0.4
Average pore size (µm)	0.17	0.12
Porosity (%)	17	14.7
Surface roughness (µm)	0.305	0.375

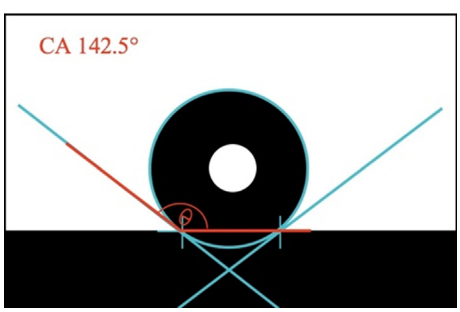

Fig. 4 Water contact angle for grafted silica sand hollow fibre ceramic membrane.

LEP value of the pristine membrane was 1.1 bar, that is due to the small size of the membrane pores (Fig. 6), which requires an additional pressure higher than the atmospheric pressure for penetration to occur; this result is in good agreement with Das et al. [30].

The three dimensions AFM images of the SSCHFM surface before and after the grafting process are shown in Fig. 5. AFM images showed an increment in the bright region after the grafting process, which illustrates an increase in the surface roughness, while the membrane's pores are seen as the dark depressions [49]. There was a noticeable increase in the surface roughness R_a of the grafted sample (from 0.305 – 0.375 µm), as seen in Fig. 5. A similar finding was also reported by Ahmad et al. on FAS-grafted ceramic membrane surfaces [50].

Pore size distribution analysis was conducted on SSCHFM before and after the surface modification process, as shown in Fig. 6. Finger-like and sponge-like pores were observed. For ungrafted SSCHFM, a pore size distribution consisting of a peak at approximately 9.64 µm representing the finger-like pores was observed. Whereas a smaller peak detected at 0.17 µm is believed to represent the sponge-like pores. After FAS grafting, the sponge-like pores peak shifted slightly to 0.11 µm, indicating that the pores became smaller. A possible explanation for this might be that the pore size became smaller due to the condensation of silanol groups and further densification of the membrane surface. During the grafting, the hydroxyl groups on the ceramic membrane surface react with Si-O-alkyl groups of the silane [51]. Garcia Fernadez et al. also obtained a slight reduction on grafted ceramic membrane pore size but neglected it due to the small gap [52]. It is interesting to note that no evident change was observed for finger-like pores after the grafting process, as shown in Fig. 2. This can be explained due to the FAS agent reacted with –OH bond on the surface pores only during FAS grafting through the immersion technique at 24 h. This result is in line with the results obtained in a previous study that observed a reduction in the sponge-like pore size of the grafted ceramic membrane, while there was no change in terms of the finger-like pore size [26].

3.2. DCMD performance

3.2.1. Effect of salt concentration

The effect of NaCl concentration on the water vapour flux of the surface grafted membrane is shown in Fig. 7. Expectedly, increases in salt concentration have decreased the permeate flux [45,53] Theoretically, the higher the concentration of a NaCl solution, the higher its boiling point. This reduces the occurrence of water evaporation on the surface of the membrane and thus will limit the amount of steam passing through the membrane [16,53]. For instance, the vapour flux reached 30 $kg/m^{2}\cdot h$ at NaCl concentration of 8 g/L, and the flux was reduced to less than half (12 $kg/m^{2}\cdot h$) when the NaCl concentration increased to 40 g/L. Three factors are believed to contribute to this observation, namely (1) the decrease in vapour

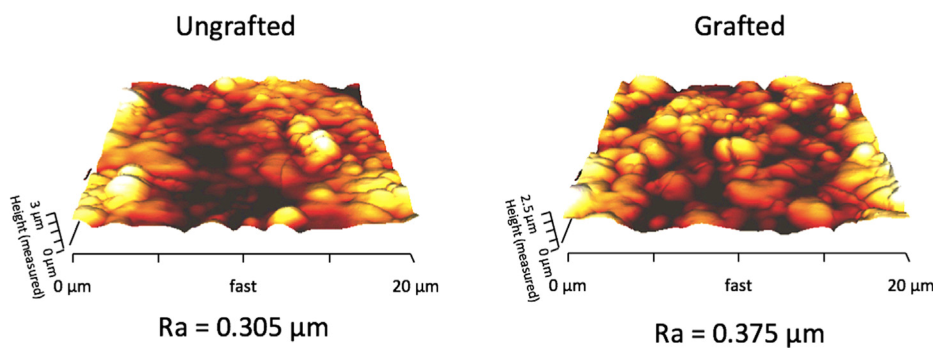

Fig. 5 Three-dimensional AFM images of ungrafted and grafted SSCHFM.

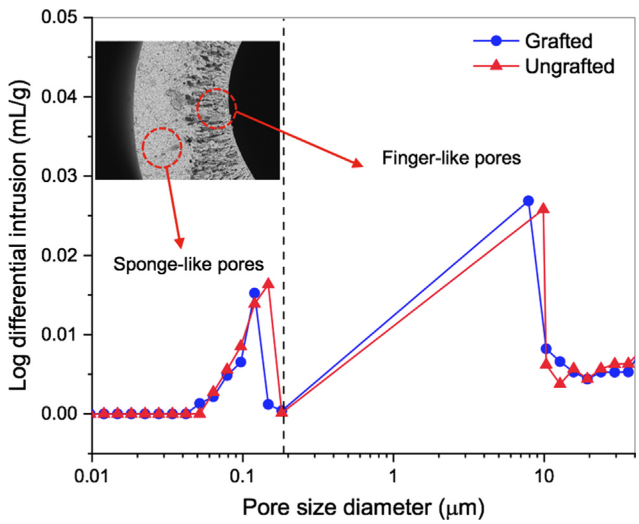

Fig. 6 Pore size distribution for SSCHFM before and after surface modification.

pressure as the salt concentration increases, (2) membrane surface fouling, and (3) concentration polarization. Regarding the first factor, it has been suggested that it is commonly experienced in the MD processes due to the activity coefficient of water being low at higher solute concentration [54]. This activity coefficient, γ_w, is expressed to the mole fraction of the solute, x_{NaCl}, as expressed in Equation (4) [55]:

$$\gamma_w = 1 - 0.5_{x_{NaCl}} - 10x_{NaCl}^2 \tag{4}$$

The value of γ_w can only be 0.466 if the value of x_{NaCl} is 0.21, translating to 450 g/L, which is higher than the solubility level of NaCl (360 g/L). The decline in flux value was mostly due to the precipitation of NaCl in response to severe concentration polarization.

3.2.2. Effect of feed temperature

A summary of the feed temperature effect on the permeate vapour flux of the surface-modified membrane is shown in Fig. 8. The difference in feed temperatures was studied while the permeate temperature was kept constant at 10 °C. A constant feed concentration of 8 g/L NaCl was used while the permeate vapour flux value of 6.3 kg/m^2·h was kept at 50 °C. An

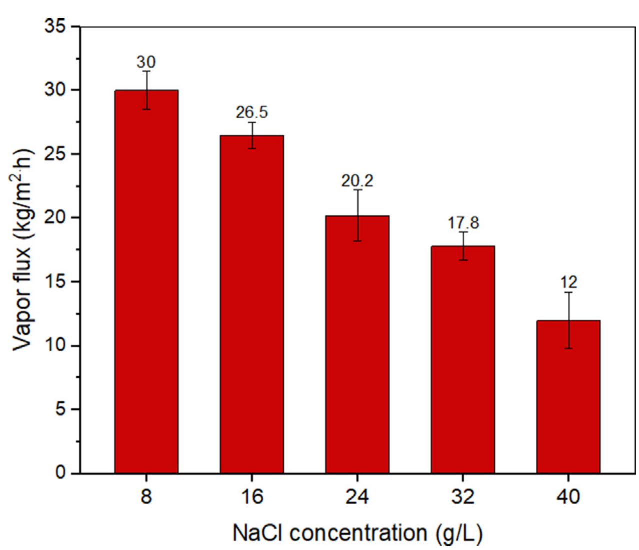

Fig. 7 Water vapour flux of grafted SSCHFM at different NaCl concentrations (10 °C permeate temperature, 80 °C feed temperature, 30 L/h feed flow rate) (number of samples, n = 3).

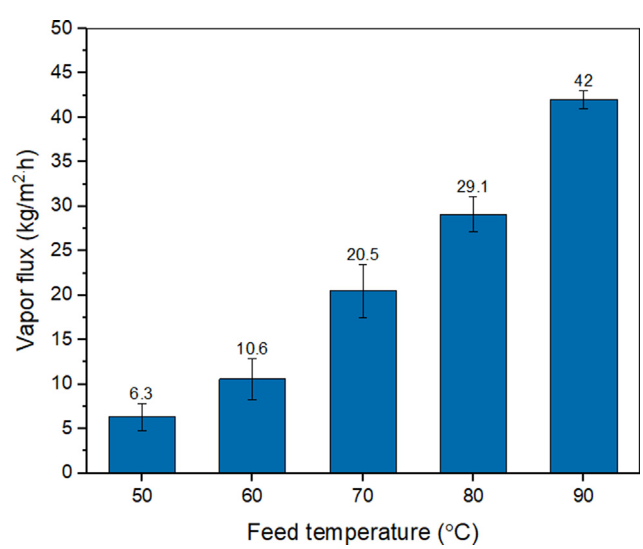

Fig. 8 Feed temperature effect on the water vapor flux of surface modified SSCHFM (NaCl concentration = 8 g/L, permeate temperature = 10 °C, feed flow rate = 30 L/h) (number of samples, n = 3).

increase in the feed temperature from 50 to 90 °C has enhanced the permeate vapour flux from 6.3 to 42 kg/m^2·h due to the increased vapour pressure [56-59]. However, this increment is not as expected, likely due to the effect of higher feed temperature on the polarization temperature. It could also be due to the increased NaCl precipitation at higher feed temperatures as there are no obvious changes in the solubility of NaCl at the studied range of temperature, while a significant change in flux is often associated with temperature increases. The permeate flux observed in this work (6.3–42 kg/m^2·h) was significantly higher than those achieved with zirconia (3.96 kg/m^2·h) and titania (0.83 kg/m^2·h) -based ceramic membranes; this study has also used a lower feed flow rate (30 L/h) comparing to 50 L/h in the previous study [3], suggesting that the prepared membrane can work well in harsh conditions and still achieve a high permeate flux.

3.2.3. Effect of feed flow rate

There is a close relationship between permeate flux and fluid dynamics, which is expected to increase at a higher feed flow rate. The relationship of feed flow and the distillate flux for the prepared SSCHFM in DCMD is shown in Fig. 9. Observably, there were increases in the permeate vapour flux with the increase of feed flow rate (from 10 to 20 L/h). Subsequently, the permeate vapour flux amplitude increased gradually from 25.8 to 39.2 kg/m^2·h, when the feed flow increased up to 60 L/h as seen in Fig. 9. This trend is due to the increase of Reynolds numbers with the increment of feed flow rate, which affected the fluid dynamics, enhancing the heat transfer coefficient and thus reducing the effect of both temperature and concentration polarization phenomenon [60]. Both mass and heat transfer resistances are reduced at higher Reynolds number, as well as the boundary layer thickness [61], this causes a more significant driving force for mass transfer through the membrane and consequently enhances the permeate of vapour flux [62]. Manuwi et al. [63] asserted that the permeate flux increased from 18.1 L/m^2·h at a flow rate of 0.5 L/min to

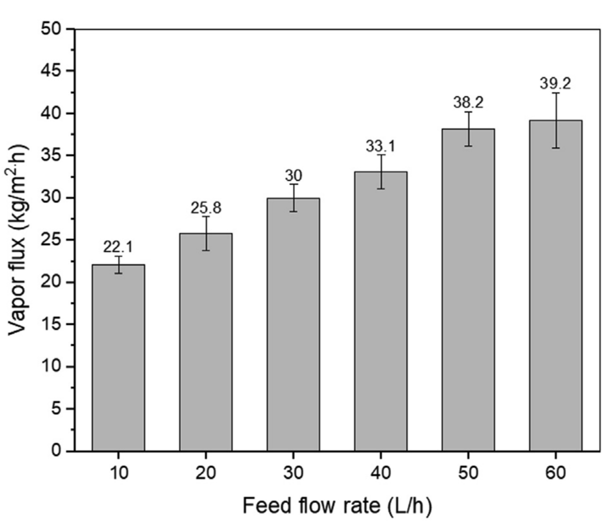

Fig. 9 Feed flow rate effect on water vapor flux of surface modified SSCHFM (feed temperature = 80 °C, permeate temperature = 10 °C, NaCl concentration = 8 g/L) (number of samples, n = 3).

29.1 L/m^2·h at a flow rate of 1.5 L/min with the same of all other parameters.

Nevertheless, it is not possible to increase the flow rate infinitely due to the increase of the pressure drop due to the increased flow rate, which occurs because of the cell walls resistance in the modules. In most cases, the pressure drop is positively proportional to the square of a flow velocity, as expressed in Equation (5) [64]. It has also been reported that permeate flux typically increases with feed flow rate, and this tends to be an asymptotic value when the feed flow rate is reasonably high [65-69].

$$\Delta P = f\frac{L}{d}\frac{u^2}{2}\rho \tag{5}$$

where ΔP is the pressure drop, f is the friction factor, L is the length of channels, d is the hydraulic diameter of the flow channel, while ρ and u are the liquid density and flow velocity, respectively.

3.2.4. Effect of the grafting process on salt rejection and water flux

The observed changes in the salt rejection capacity and vapour flux of the grafted SSCHFM during DCMD operation for 32 h were presented in Fig. 10. The process was conducted at a feed temperature of 80 °C and a feed flow rate of 30 L/h, using NaCl (8 g/L) as the feed solution. Initially, a permeate vapour flux of 35 kg/m^{2}h was recorded. Subsequently, a decline in permeate vapour was observed to 27 kg/m^2·h after 24 h of the operation. Whereas the grafted SSCHFM exhibited a salt rejection rate of 100%. Table 3 presents a comparison of the vapour fluxes and salt rejection levels of the grafted membrane in this study with those of grafted ceramic and polymeric membranes reported in the previous studies. It can be observed that the grafted SSCHFM exhibited an excellent Initial vapour flux of 35 kg/m^2·h, which is much higher compared to those in the previous studies [3,57,70]. In terms of durability performance, a 32 h membrane distillation process has been performed. Upon the test, the rejection rate presented no dependence with the NaCl concentration, as observed in Fig. 10. Therefore the performance showed no reduction throughout the process (100% of salt rejection); this result is in good agreement with experimental observations [53], while there were no significant fluctuations exhibited in the membrane flux from hour 24 towards the end of the performance test, which indicates that the membrane is highly durable in terms of hydrophobic coating (surface modification), membrane structure (break or brittleness) and performance of rejection.

The contact angle of water is a direct measure of the membrane's hydrophobicity behaviour which is a key in any MD process for repelling the feed solution liquid from penetrating the membrane [71]. To determine the hydrophobic layer stability of the modified membrane, the contact angle of SSCHFM before and after 32 h of the DCMD test was measured (Fig. 10). There was barely change observed on the contact angle value of the modified SSCHFM; the contact angle value was slightly decreased from 142.5° to 141°. To be more precise, the reduction percentage was less than 1%. This result is in good agreement with the finding of a previous study that observed a reduction in water contact angle of hydrophobic polytetrafluoroethylene membrane from 134.78° to 129.8° after the DCMD test [71]. Hubadillah et al. [26] studied the

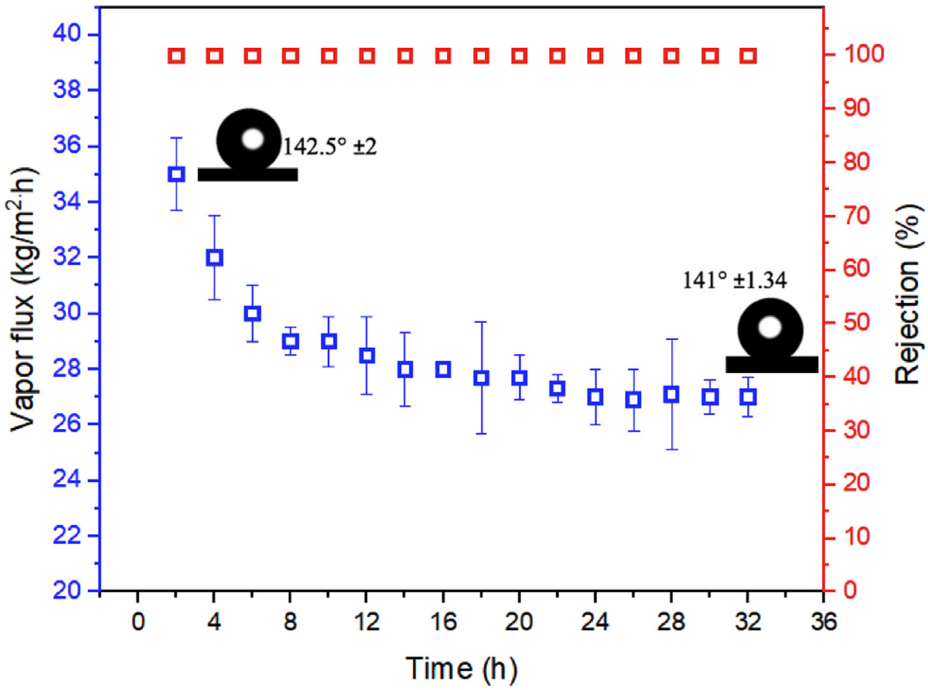

Fig. 10 Water vapour flux and NaCl rejection of the grafted membrane at 80 °C feed temperature, 10 °C permeate temperature, 8 g/L NaCl concentration, 30 L/h feed flow rate; and the water contact angle before and after DCMD (number of samples, n = 3).

Table 3 Benchmarking the observed salt rejection and permeate flux performances with the existing literature values for grafted membranes applied in MD process.

Membrane configuration	Material of membrane	FAS silane	Contact angle (°)	NaCl concentration (g/L)	Permeate vapor flux ($kg/m^2.h$)	Rejection (%)	Ref
Hollow fibre	Titania	1H, 1H,2H, 2H-Perfluorooctyltrie-thoxysilane	135-145	30	0.9–3.0	> 99.1	[72]
Hollow fibre	Mullite	1H,1H,2H,2H–Perfluorodecyltrie-thoxysilane	139	10	11.79	99.99	[16]
Hollow fibre	β-Sialon	1H,1H,2H,2H–Perfluorodecyltrie-thoxysilane	125	20	6.79	99	[43]
Hollow fibre	Silicon nitride	1H, 1H, 2H, 2H-perfluorooctyltrie-thoxysilane,	136	5–60	7.83–22.4	99–100	[73]
Hollow fibre	PVDF	–	100.81		16	99.9	[70]
Hollow fibre	PC/PVDF	–	150	35	8.1	99.9	[74]
Hollow fibre	MOF/PVDF	–	–	10	11	99.9	[75]
Hollow fibre	PTFE/PVDF	–	136.5	35	26.8	99.9	[76]
Hollow fibre	Silica sand	1H,1H,2H,2H–Perfluorodecyltriethoxysilane	142.5	8–40	12–35	100	This work

arsenic removal from aqueous solution via direct contact membrane distillation using hydrophobic kaolin hollow fibre membrane; the kaolin membrane was modified using FAS agent through the immersion method. The study showed that the water contact angle was insignificantly decreased by 4° after 8 h of operation. It is noteworthy that in this current work, the decrement of the contact angle value was only 1.5° during 32 h of the operation, which indicates that the surface modification of SSCHFM is thermally stable compared to studies in the literature.

4. Cost analysis of hydrophobic SSHFCM

The estimated cost of fabricating SSHFCM was computed in this section. The cost estimation considered two significant components: (1) raw material costs and (2) energy usage expenses. **Supplementary Information** contains an example of cost calculations for membrane fabrication. It is well established that alumina membranes are the most used ceramic membranes for water separation [77,78]. Additionally, kaolin has been extensively investigated as a potential alternative

Table 4 Cost of raw materials and energy consumption estimations of the fabrications of the HFCMs developed from three different starting ceramic materials.

	Silica sand HFCM	Alumina HFCM [81,83]	Kaolin HFCM [82]
Total raw material cost ($/m^2 HFCM)	88.40	190.7	106.2
Total energy consumption for membrane fabrication (kWh/m^2 HFCM)	0.318	0.340	0.326
Cost of energy consumed ($/m^2 HFCM)	0.0349	0.0374	0.0358
Total raw material (surface modification) cost ($/m^2 HFCM)	242.71	242.71	242.71

Remark: 1. The calculations were based on 1 m^2 HFCM as the basis.
2. The estimated fabrication costs of the alumina and kaolin HFCMs were calculated by referring to the fabrication conditions.

material for developing cost-effective ceramic membranes [79,80]. Thus, alumina and kaolin hollow fiber ceramic membranes (HFCMs) were used as cost standards in this study. The estimated fabrication costs of the alumina and kaolin HFCMs were calculated by referring to the fabrication conditions reported in the literature [81,82]. Table 4 summarises the estimated costs and energy consumption associated with fabricating these three membranes.

The use of silica sand as a low-cost starting material significantly reduced the membrane fabrication's overall raw material cost. The overall cost of raw materials used to fabricate the SSHFCM was $ 88.40/m^2 HFCM, which was 53.6% and 16.7% less than the costs of alumina and kaolin HFCMs, respectively. Due to the SSHFCM's lower sintering temperature, the sintering stage consumed 6.68% and 2.51% less energy than the alumina and kaolin HFCMs, respectively. The findings of the cost analysis indicate that the primary factor affecting the cost of fabricating ceramic membranes is the cost of raw materials. As a result, the use of low-cost starting ceramic material is crucial to minimize the fabrication cost of ceramic membranes. The surface modification step showed no notable improvement in the total since the three membranes were grafted using the same concentration of FAS agent (2 wt%).

5. Conclusions

This work reported the fabrication of low-cost SSCHFM from natural silica sand using phase inversion and sintering technique. The SSCHFMs were characterized using SEM, AFM, contact angle, LEPw, and MIP. It was proved that the hydrophilic character of ceramic silica sand membrane could be changed into a hydrophobic by surface modification using 1H,1H,2H,2H perfluorodecyltriethoxysilane (FAS17) for DCMD application. The grafting process impacted the SSHFCM by the increase in the water contact angles of the membrane (142.5°) and its LEPw value (>2.6 bar). AFM images showed an increment in the surface roughness of the grafted SSCHFM from 0.305 µm to 0.375 µm, with a slight decrease in the average pore size and porosity from 0.17 µm and 17% to 0.12 µm and 14.7% respectively. The performance of the grafted SSCHFM on DCMD processes was evaluated for 32 h using 8 g/L NaCl as the feed solution. Notably, the samples achieved excellent salt rejection of 100% and excellent water flux (35 kg/m^2·h) performances. Further, studies on the effect of feed flow rate, feed temperature, and salt concentration on the water vapour flux were also performed and as expected, declines trends were observed in the flux at higher salt concentrations. In contrast, increments were recorded in the flux with the feed flow rate and feed temperature increase. Therefore, this study could be a valuable way of producing high-performing membranes for use in DCMD processes. Furthermore, the prepared membrane can also be used in the removal of heavy metals from the water via DCMD processes as being currently investigated.

Declaration of Competing Interest

The authors declare that they have no known competing financial interests or personal relationships that could have appeared to influence the work reported in this paper.

Acknowledgement

Funding: The authors gratefully acknowledge the financial support from the Ministry of Higher Education Malaysia under the Higher Institution Centre of Excellence Scheme (Project Number: R.J090301.7851.4J427) and Malaysia Research University Network (MRUN) Grant (Project Number: R.J130000.7809.4L867), Ministry of Science, Technology and Innovation (MOSTI) Malaysia under International Collaboration Fund (ICF) (Project Number: IF0120I1164 / R.J130000.7909.4S145), and Universiti Teknologi Malaysia under the Matching Grant (Project number: Q.J130000.3009.03 M15) and Collaborative Research Grant (CRG) (Project number: Q.J130000.2409.08G29). The author also would like to thank JICA Technical Cooperation Project for ASEAN University Network/Southeast Asia Engineering Education Development Network (JICA Project for AUN/SEED-Net) via Collaborative Education Program (Project number: UTM CEP 2102a / R.J130000.7309.4B647).

Appendix A. Supplementary material

Supplementary data to this article can be found online at https://doi.org/10.1016/j.aej.2022.03.044.

References

[1] Y. Tokui, H. Moriguchi, Y. Nishi, Comprehensive environmental assessment of seawater desalination plants: Multistage flash distillation and reverse osmosis membrane types in Saudi Arabia, Desalination 351 (2014) 145–150, https://doi.org/10.1016/j.desal.2014.07.034.

[2] M. S. A. Kader, P. Karthikeyan, and C. Ramnath, "SEA WATER DESALINATION BY THERMAL METHOD," vol. 03, no. 01, pp. 59–62, 2017.

[3] S. Cerneaux, I. Struzyńska, W.M. Kujawski, M. Persin, A. Larbot, Comparison of various membrane distillation methods for desalination using hydrophobic ceramic membranes, J. Memb. Sci. 337 (1–2) (2009) 55–60, https://doi.org/10.1016/j.memsci.2009.03.025.

[4] A. Alkhudhiri, N. Darwish, N. Hilal, Membrane distillation: A comprehensive review, Desalination 287 (2012) 2–18, https://doi.org/10.1016/j.desal.2011.08.027.

[5] A. Boubakri, S.A.T. Bouguecha, I. Dhaouadi, A. Hafiane, Effect of operating parameters on boron removal from seawater using membrane distillation process, Desalination 373 (2015) 86–93, https://doi.org/10.1016/j.desal.2015.06.025.

[6] E. Drioli, A. Ali, S. Simone, F. Macedonio, S.A. AL-Jlil, F.S. Al Shabonah, H.S. Al-Romaih, O. Al-Harbi, A. Figoli, A. Criscuoli, Novel PVDF hollow fiber membranes for vacuum and direct contact membrane distillation applications, Sep. Purif. Technol. 115 (2013) 27–38, https://doi.org/10.1016/j.seppur.2013.04.040.

[7] J.A. Prince, D. Rana, G. Singh, T. Matsuura, T. Jun Kai, T.S. Shanmugasundaram, Effect of hydrophobic surface modifying macromolecules on differently produced PVDF membranes for direct contact membrane distillation, Chem. Eng. J. 242 (2014) 387–396, https://doi.org/10.1016/j.cej.2013.11.039.

[8] G. Kang, Y. Cao, Application and modification of poly (vinylidene fluoride) (PVDF) membranes – A review, J. Memb. Sci. 463 (2014) 145–165, https://doi.org/10.1016/j.memsci.2014.03.055.

[9] Z. Jin, D.L. Yang, S.H. Zhang, X.G. Jian, Hydrophobic modification of poly(phthalazinone ether sulfone ketone) hollow fiber membrane for vacuum membrane distillation, J. Memb. Sci. 310 (1) (2008) 20–27, https://doi.org/10.1016/j.memsci.2007.10.021.

[10] S. Devi, P. Ray, K. Singh, P.S. Singh, Preparation and characterization of highly micro-porous PVDF membranes for desalination of saline water through vacuum membrane distillation, Desalination 346 (2014) 9–18, https://doi.org/10.1016/j.desal.2014.05.004.

[11] L. Lin, H. Geng, Y. An, P. Li, H. Chang, Preparation and properties of PVDF hollow fiber membrane for desalination using air gap membrane distillation, Desalination 367 (2015) 145–153, https://doi.org/10.1016/j.desal.2015.04.005.

[12] S.L. Sandhya Rani, R.V. Kumar, "Insights on applications of low-cost ceramic membranes in wastewater treatment: A mini-review", Case Stud. Chem. Environ. Eng. 4 (2021) 100149, https://doi.org/10.1016/j.cscee.2021.100149.

[13] M. Cha, C. Boo, C. Park, Simultaneous retention of organic and inorganic contaminants by a ceramic nanofiltration membrane for the treatment of semiconductor wastewater, Process Saf. Environ. Prot. 159 (2022) 525–533, https://doi.org/10.1016/j.psep.2022.01.032.

[14] Y.H. Teow, Y.H. Chiah, K.C. Ho, E. Mahmoudi, Treatment of semiconductor-industry wastewater with the application of ceramic membrane and polymeric membrane, J. Clean. Prod. 337 (2022) 130569, https://doi.org/10.1016/j.jclepro.2022.130569.

[15] Z.S. Tai, M.H.D. Othman, A. Mustafa, J. Ravi, K.C. Wong, K. N. Koo, S.K. Hubadillah, M.A. Azali, N.H. Alias, B.C. Ng, M. I.H. Mohamed Dzahir, A.F. Ismail, M.A. Rahman, J. Jaafar, Development of hydrophobic polymethylhydrosiloxane/tetraethylorthosilicate (PMHS/TEOS) hybrid coating on ceramic membrane for desalination via membrane distillation, J. Memb. Sci. 637 (2021) 119609, https://doi.org/10.1016/j.memsci.2021.119609.

[16] M.F. Twibi, M.H.D. Othman, S.K. Hubadillah, S.A. Alftessi, M.R.B. Adam, A.F. Ismail, M.A. Rahman, J. Jaafar, Y.O. Raji, M.H. Abd Aziz, M.N.B.M. Sokri, H. Abdullah, R. Naim, Hydrophobic mullite ceramic hollow fibre membrane (Hy-MHFM) for seawater desalination via direct contact membrane distillation (DCMD), J. Eur. Ceram. Soc. 41 (13) (2021) 6578–6585, https://doi.org/10.1016/j.jeurceramsoc.2021.06.024.

[17] K. Bin Bandar, M. D. Alsubei, S. A. Aljlil, N. Bin Darwish, and N. Hilal, "Membrane distillation process application using a novel ceramic membrane for Brackish water desalination," *Desalination*, vol. 500, no. December 2020, p. 114906, 2021, doi: 10.1016/j.desal.2020.114906.

[18] M.H. Abd Aziz, M.A.B. Pauzan, N.A.S. Mohd Hisam, M.H.D. Othman, M.R. Adam, Y. Iwamoto, M. Hafiz Puteh, M.A. Rahman, J. Jaafar, A. Fauzi Ismail, T. Agustiono Kurniawan, S. Abu Bakar, Superhydrophobic ball clay based ceramic hollow fibre membrane via universal spray coating method for membrane distillation, Sep. Purif. Technol. 288 (2022) 120574, https://doi.org/10.1016/j.seppur.2022.120574.

[19] S. Freeman, H. Shorney-Darby, What's the Buzz About Ceramic Membranes?, J Am. Water Works Assoc. 103 (12) (2011) 12–13, https://doi.org/10.1002/j.1551-8833.2011.tb11572.x.

[20] S.K. Hubadillah, M.H.D. Othman, A.F. Ismail, M.A. Rahman, J. Jaafar, Y. Iwamoto, S. Honda, M.I.H.M. Dzahir, M.Z.M. Yusop, Fabrication of low cost, green silica based ceramic hollow fibre membrane prepared from waste rice husk for water filtration application, Ceram. Int. 44 (9) (2018) 10498–10509, https://doi.org/10.1016/j.ceramint.2018.03.067.

[21] S.K. Hubadillah, Z. Harun, M.H.D. Othman, A.F. Ismail, W. N.W. Salleh, H. Basri, M.Z. Yunos, P. Gani, Preparation and characterization of low cost porous ceramic membrane support from kaolin using phase inversion/sintering technique for gas separation: Effect of kaolin content and non-solvent coagulant bath, Chem. Eng. Res. Des. 112 (2016) 24–35, https://doi.org/10.1016/j.cherd.2016.06.007.

[22] L. Li, M. Chen, Y. Dong, X. Dong, S. Cerneaux, S. Hampshire, J. Cao, L.i. Zhu, Z. Zhu, J. Liu, A low-cost alumina-mullite composite hollow fiber ceramic membrane fabricated via phase-inversion and sintering method, J. Eur. Ceram. Soc. 36 (8) (2016) 2057–2066, https://doi.org/10.1016/j.jeurceramsoc.2016.02.020.

[23] S.A. Alftessi, M.H.D. Othman, M.R. Adam, T.M. Farag, A.F. Ismail, M.A. Rahman, J. Jaafar, M.A. Habib, Y.O. Raji, S.K. Hubadillah, Novel silica sand hollow fibre ceramic membrane for oily wastewater treatment, J. Environ. Chem. Eng. 9 (1) (2021) 104975, https://doi.org/10.1016/j.jece:2020.104975.

[24] M.F. Twibi, M.H.D. Othman, S.K. Hubadillah, S.A. Alftessi, T. A. Kurniawan, A.F. Ismail, M.A. Rahman, J. Jaafar, Y.O. Raji, Development of high strength, porous mullite ceramic hollow fiber membrane for treatment of oily wastewater, Ceram. Int. 47 (11) (2021) 15367–15382, https://doi.org/10.1016/j.ceramint.2021.02.102.

[25] W. K. b Andre Larbot a*, Laetitia Gazagnes a, Sebastian Krajewski b, Malgorzata Bukowska b and AInstitut, "Water desalination using ceramic membrane distillation," vol. 168, no. C, pp. 367–372, 2004.

[26] S.K. Hubadillah, M.H.D. Othman, A.F. Ismail, M.A. Rahman, J. Jaafar, A low cost hydrophobic kaolin hollow fiber membrane (h-KHFM) for arsenic removal from aqueous solution via direct contact membrane distillation, Separat. Purificat. Technol. 214 (2019) 31–39.

[27] I. Hedfi, N. Hamdi, M.A. Rodriguez, E. Srasra, Development of a low cost micro-porous ceramic membrane from kaolin and Alumina, using the lignite as porogen agent, Ceram. Int. 42 (4) (2016) 5089–5093, https://doi.org/10.1016/j.ceramint.2015.12.023.

[28] A. Kasprzhitskii, G. Lazorenko, V. Yavna, P. Daniel, DFT theoretical and FT-IR spectroscopic investigations of the plasticity of clay minerals dispersions, J. Mol. Struct. 1109 (2016) 97–105, https://doi.org/10.1016/j.molstruc.2015.12.064.

[29] R.V. Kumar, L. Goswami, K. Pakshirajan, G. Pugazhenthi, Dairy wastewater treatment using a novel low cost tubular ceramic membrane and membrane fouling mechanism using pore blocking models, J. Water Process Eng. 13 (2016) 168–175, https://doi.org/10.1016/j.jwpe.2016.08.012.

[30] R. Das, K. Sondhi, S. Majumdar, S. Sarkar, Development of hydrophobic clay–alumina based capillary membrane for desalination of brine by membrane distillation, J. Asian Ceram. Soc. 4 (3) (2016) 243–251, https://doi.org/10.1016/j.jascer.2016.04.004.

[31] S.K. Hubadillah, M.H.D. Othman, T. Matsuura, M.A. Rahman, J. Jaafar, A.F. Ismail, S.Z.M. Amin, Green silica-based ceramic hollow fiber membrane for seawater desalination via direct contact membrane distillation, Sep. Purif. Technol. 205 (2018) 22–31, https://doi.org/10.1016/j.seppur.2018.04.089.

[32] M.R. Jamalludin, Z. Harun, M.H.D. Othman, S.K. Hubadillah, M.Z. Yunos, A.F. Ismail, Morphology and property study of green ceramic hollow fiber membrane derived from waste sugarcane bagasse ash (WSBA), Ceram. Int. 44 (15) (2018) 18450–18461, https://doi.org/10.1016/j.ceramint.2018.07.063.

[33] N.H. Kamarudin, Z. Harun, M.H.D. Othman, T. Abdullahi, S. Syamsul Bahri, N.H. Kamarudin, M.Z. Yunos, W.N. Wan Salleh, Waste environmental sources of metakaolin and corn cob ash for preparation and characterisation of green ceramic hollow fibre membrane (h-MCa) for oil-water separation, Ceram. Int. 46 (2) (2020) 1512–1525, https://doi.org/10.1016/j.ceramint.2019.09.118.

[34] L. Wang, G. Skjevrak, J.E. Hustad, M. Grønli, Ø. Skreiberg, Effects of additives on barley straw and husk ashes sintering characteristics, Energy Procedia 20 (1876) (2012) 30–39, https://doi.org/10.1016/j.egypro.2012.03.005.

[35] Z.S. Tai, S.K. Hubadillah, M.H.D. Othman, M.I.H.M. Dzahir, K.N. Koo, N.I.S.T.I. Tendot, A.F. Ismail, M.A. Rahman, J. Jaafar, M.H.A. Aziz, Influence of pre-treatment temperature of palm oil fuel ash on the properties and performance of green ceramic hollow fiber membranes towards oil/water separation application, Sep. Purif. Technol. 222 (2019) 264–277, https://doi.org/10.1016/j.seppur.2019.04.046.

[36] L.T. Yogarathinam, J. Usman, M.H.D. Othman, A.F. Ismail, P. S. Goh, A. Gangasalam, M.R. Adam, Low-cost silica based ceramic supported thin film composite hollow fiber membrane from guinea corn husk ash for efficient removal of microplastic from aqueous solution, J. Hazard. Mater. 424 (2022) 127298, https://doi.org/10.1016/j.jhazmat.2021.127298.

[37] Z.D. Hendren, J. Brant, M.R. Wiesner, Surface modification of nanostructured ceramic membranes for direct contact membrane distillation, J. Memb. Sci. 331 (1) (2009) 1–10, https://doi.org/10.1016/j.memsci.2008.11.038.

[38] C.P. Tripp, M.L. Hair, An Infrared Study of the Reaction of Octadecyltrichlorosilane with Silica, Langmuir 8 (4) (1992) 1120–1126, https://doi.org/10.1021/la00040a018.

[39] K.J. Lu, Y. Chen, T.S. Chung, Design of omniphobic interfaces for membrane distillation – A review, Water Res. 162 (2019) 64–77, https://doi.org/10.1016/j.watres.2019.06.056.

[40] M. Khemakhem, S. Khemakhem, R. Ben Amar, Emulsion separation using hydrophobic grafted ceramic membranes by, Colloids Surfaces A Physicochem. Eng. Asp. 436 (2013) 402–407, https://doi.org/10.1016/j.colsurfa.2013.05.073.

[41] Z. Qiao, Z. Wang, C. Zhang, S. Yuan, Y. Zhu, J. Wang, S. Wang, PVAm–PIP/PS composite membrane with high performance for CO 2/N 2 separation, AIChE J. 59 (1) (2013) 215–228.

[42] J.-W. Wang, X.-Z. Li, M. Fan, J.-Q. Gu, L.-Y. Hao, X. Xu, C.-S. Chen, C.-M. Wang, Y.-Z. Hao, S. Agathopoulos, Porous β-Sialon planar membrane with a robust polymer-derived hydrophobic ceramic surface, J. Memb. Sci. 535 (2017) 63–69, https://doi.org/10.1016/j.memsci.2017.04.028.

[43] J.W. Wang, L. Li, J.W. Zhang, X. Xu, C.S. Chen, β-Sialon ceramic hollow fiber membranes with high strength and low thermal conductivity for membrane distillation, J. Eur. Ceram. Soc. 36 (1) (2016) 59–65, https://doi.org/10.1016/j.jeurceramsoc.2015.09.027.

[44] J. Kujawa, W. Kujawski, S. Koter, K. Jarzynka, A. Rozicka, K. Bajda, S. Cerneaux, M. Persin, A. Larbot, Membrane distillation properties of TiO2 ceramic membranes modified by perfluoroalkylsilanes, Desalin. Water Treat. 51 (7-9) (2013) 1352–1361, https://doi.org/10.1080/19443994.2012.704976.

[45] S.R. Krajewski, W. Kujawski, M. Bukowska, C. Picard, A. Larbot, Application of fluoroalkylsilanes (FAS) grafted ceramic membranes in membrane distillation process of NaCl solutions, J. Memb. Sci. 281 (1–2) (2006) 253–259, https://doi.org/10.1016/j.memsci.2006.03.039.

[46] G. Rácz, S. Kerker, Z. Kovács, G. Vatai, M. Ebrahimi, P. Czermak, Theoretical and experimental approaches of liquid entry pressure determination in membrane distillation processes, Period. Polytech. Chem. Eng. 58 (2) (2014) 81–91, https://doi.org/10.3311/PPch.2179.

[47] M. Mulder, Basic principles of membrane technology, Springer Science & Business Media, 2012.

[48] E. Drioli, V. Calabro, Y. Wu, Microporous Membranes in Membrane Distillation, Pure Appl. Chem. 58 (12) (1986) 1657–1662, https://doi.org/10.1351/pac198658121657.

[49] N. Yusof, D. Rana, A.F. Ismail, T. Matsuura, Microstructure of polyacrylonitrile-based activated carbon fibers prepared from solvent-free coagulation process, J. Appl. Res. Technol. 14 (1) (2016) 54–61, https://doi.org/10.1016/j.jart.2016.02.001.

[50] N.A. Ahmad, C.P. Leo, A.L. Ahmad, Superhydrophobic alumina membrane by steam impingement: Minimum resistance in microfiltration, Sep. Purif. Technol. 107 (2013) 187–194, https://doi.org/10.1016/j.seppur.2013.01.011.

[51] M. Khemakhem, S. Khemakhem, R. Ben Amar, Surface modification of microfiltration ceramic membrane by fluoroalkylsilane, Desalin. Water Treat. 52 (7–9) (2014) 1786–1791, https://doi.org/10.1080/19443994.2013.807023.

[52] L. García-Fernández, B. Wang, M.C. García-Payo, K. Li, M. Khayet, Morphological design of alumina hollow fiber membranes for desalination by air gap membrane distillation, Desalination 420 (March) (2017) 226–240, https://doi.org/10.1016/j.desal.2017.07.021.

[53] L. Gazagnes, S. Cerneaux, M. Persin, E. Prouzet, A. Larbot, Desalination of sodium chloride solutions and seawater with hydrophobic ceramic membranes, Desalination 217 (1–3) (2007) 260–266, https://doi.org/10.1016/j.desal.2007.01.017.

[54] H. Liu, J. Wang, Treatment of radioactive wastewater using direct contact membrane distillation, J. Hazard. Mater. 261 (2013) 307–315, https://doi.org/10.1016/j.jhazmat.2013.07.045.

[55] M. Tomaszewska, Direct Contact Membrane Distillation (DCMD), Applications (2016).

[56] H. Zhu, H. Wang, F. Wang, Y. Guo, H. Zhang, J. Chen, Preparation and properties of PTFE hollow fiber membranes for desalination through vacuum membrane distillation, J. Memb. Sci. 446 (2013) 145–153, https://doi.org/10.1016/j.memsci.2013.06.037.

[57] J.-M. Li, Z.-K. Xu, Z.-M. Liu, W.-F. Yuan, H. Xiang, S.-Y. Wang, Y.-Y. Xu, Microporous polypropylene and polyethylene hollow fiber membranes. Part 3. Experimental studies on membrane distillation for desalination, Desalination 155 (2) (2003) 153–156, https://doi.org/10.1016/S0011-9164(03)00292-3.

[58] J. Koo, J. Han, J. Sohn, S. Lee, T.M. Hwang, Experimental comparison of direct contact membrane distillation (DCMD) with vacuum membrane distillation (VMD), Desalin. Water Treat. 51 (31–33) (2013) 6299–6309, https://doi.org/10.1080/19443994.2013.780817.

[59] B.B. Ashoor, S. Mansour, A. Giwa, V. Dufour, S.W. Hasan, Principles and applications of direct contact membrane

distillation (DCMD): A comprehensive review, Desalination 398 (2016) 222–246, https://doi.org/10.1016/j.desal.2016.07.043.
[60] P. Pal, A.K. Manna, Removal of arsenic from contaminated groundwater by solar-driven membrane distillation using three different commercial membranes, Water Res. 44 (19) (2010) 5750–5760, https://doi.org/10.1016/j.watres.2010.05.031.
[61] M.C. García-Payo, M.A. Izquierdo-Gil, C. Fernández-Pineda, Air gap membrane distillation of aqueous alcohol solutions, J. Memb. Sci. 169 (1) (2000) 61–80, https://doi.org/10.1016/S0376-7388(99)00326-9.
[62] L. Chen, P. Xu, and H. Wang, ‘‘Interplay of the factors affecting water flux and salt rejection in membrane distillation: A state-of-the-art critical review,’’ *Water (Switzerland)*, vol. 12, no. 10, 2020, doi: 10.3390/w12102841.
[63] Y.M. Manawi, M. Khraisheh, A.K. Fard, F. Benyahia, S. Adham, Effect of operational parameters on distillate flux in direct contact membrane distillation (DCMD): Comparison between experimental and model predicted performance, Desalination 336 (1) (2014) 110–120, https://doi.org/10.1016/j.desal.2014.01.003.
[64] J.P. Holman, Heat Transfer, Tenth ed., McGraw-Hill, New York, 2010.
[65] S. Srisurichan, R. Jiraratananon, A.G. Fane, Mass transfer mechanisms and transport resistances in direct contact membrane distillation process, J. Memb. Sci. 277 (1–2) (2006) 186–194, https://doi.org/10.1016/j.memsci.2005.10.028.
[66] X. Yang, R. Wang, A.G. Fane, Novel designs for improving the performance of hollow fiber membrane distillation modules, J. Memb. Sci. 384 (1–2) (2011) 52–62, https://doi.org/10.1016/j.memsci.2011.09.007.
[67] H.J. Hwang, K. He, S. Gray, J. Zhang, I.S. Moon, Direct contact membrane distillation (DCMD): Experimental study on the commercial PTFE membrane and modeling, J. Memb. Sci. 371 (1–2) (2011) 90–98, https://doi.org/10.1016/j.memsci.2011.01.020.
[68] X. Yang, R. Wang, L. Shi, A.G. Fane, M. Debowski, Performance improvement of PVDF hollow fiber-based membrane distillation process, J. Memb. Sci. 369 (1–2) (2011) 437–447, https://doi.org/10.1016/j.memsci.2010.12.020.
[69] M.A. Izquierdo-Gil, C. Fernández-Pineda, M.G. Lorenz, Flow rate influence on direct contact membrane distillation experiments: Different empirical correlations for Nusselt number, J. Memb. Sci. 321 (2) (2008) 356–363, https://doi.org/10.1016/j.memsci.2008.05.018.
[70] Y. Tang, N. Li, A. Liu, S. Ding, C. Yi, H. Liu, Effect of spinning conditions on the structure and performance of hydrophobic PVDF hollow fiber membranes for membrane distillation, Desalination 287 (2012) 326–339, https://doi.org/10.1016/j.desal.2011.11.045.
[71] H. Abdelrazeq, M. Khraisheh, F. Al Momani, J.T. McLeskey, M.K. Hassan, M. Gad-el-Hak, H.V. Tafreshi, Performance of electrospun polystyrene membranes in synthetic produced industrial water using direct-contact membrane distillation, Desalination 493 (2020) 114663, https://doi.org/10.1016/j.desal.2020.114663.
[72] J. Kujawa, S. Cerneaux, S. Koter, W. Kujawski, Highly efficient hydrophobic titania ceramic membranes for water desalination, ACS Appl. Mater. Interfaces 6 (16) (2014) 14223–14230, https://doi.org/10.1021/am5035297.
[73] J.W. Zhang, H. Fang, J.W. Wang, L.Y. Hao, X. Xu, C.S. Chen, Preparation and characterization of silicon nitride hollow fiber membranes for seawater desalination, J. Memb. Sci. 450 (2014) 197–206, https://doi.org/10.1016/j.memsci.2013.08.042.
[74] C. Fang, W. Liu, P. Zhang, M. Yao, S. Rajabzadeh, N. Kato, H. o. Kyong Shon, H. Matsuyama, Controlling the inner surface pore and spherulite structures of PVDF hollow fiber membranes in thermally induced phase separation using triple-orifice spinneret for membrane distillation, Sep. Purif. Technol. 258 (2021) 117988, https://doi.org/10.1016/j.seppur.2020.117988.
[75] D. Cheng, L. Zhao, N.a. Li, S.J.D. Smith, D. Wu, J. Zhang, D. Ng, C. Wu, M.R. Martinez, M.P. Batten, Z. Xie, Aluminum fumarate MOF/PVDF hollow fiber membrane for enhancement of water flux and thermal efficiency in direct contact membrane distillation, J. Memb. Sci. 588 (2019) 117204, https://doi.org/10.1016/j.memsci.2019.117204.
[76] W. Shi, T. Li, M. Fan, H. Li, H. Zhang, X. Qin, Construction of rough and porous surface of hydrophobic PTFE powder-embedded PVDF hollow fiber composite membrane for accelerated water mass transfer of membrane distillation, J. Industrial Eng. Chem. 108 (2022) 328–343.
[77] Y. Yang, Q. Chang, Z. Hu, and X. Zhang, ‘‘A Comparative Study on the Addition Methods of TiO2 Sintering Aid to the Properties of Porous Alumina Membrane Support,’’ *Membranes (Basel)*., vol. 8, no. 3, 2018, doi: 10.3390/membranes8030049.
[78] B. Wang, ‘‘Alumina Membranes,’’ in *Encyclopedia of Membranes*, E. Drioli and L. Giorno, Eds. Berlin, Heidelberg: Springer Berlin Heidelberg, 2015, pp. 1–2.
[79] A. Agarwalla, K. Mohanty, Comprehensive characterization, development, and application of natural/Assam Kaolin-based ceramic microfiltration membrane, Mater. Today Chem. 23 (2022) 100649, https://doi.org/10.1016/j.mtchem.2021.100649.
[80] S.K. Hubadillah, M.H.D. Othman, T. Matsuura, A.F. Ismail, M.A. Rahman, Z. Harun, J. Jaafar, M. Nomura, Fabrications and applications of low cost ceramic membrane from kaolin: A comprehensive review, Ceram. Int. 44 (5) (2018) 4538–4560, https://doi.org/10.1016/j.ceramint.2017.12.215.
[81] B.F.K. Kingsbury, K. Li, A morphological study of ceramic hollow fibre membranes, J. Memb. Sci. 328 (1–2) (2009) 134–140, https://doi.org/10.1016/j.memsci.2008.11.050.
[82] S. K. Hubadillah, M. H. D. Othman, A. F. Ismail, M. A. Rahman, and J. Jaafar, ‘‘A low cost hydrophobic kaolin hollow fiber membrane (h-KHFM) for arsenic removal from aqueous solution via direct contact membrane distillation,’’ *Sep. Purif. Technol.*, vol. 214, no. February 2018, pp. 31–39, 2019, doi: 10.1016/j.seppur.2018.04.025.
[83] C. Ren, H. Fang, J. Gu, L. Winnubst, C. Chen, Preparation and characterization of hydrophobic alumina planar membranes for water desalination, J. Eur. Ceram. Soc. 35 (2) (2015) 723–730, https://doi.org/10.1016/j.jeurceramsoc.2014.07.012.